Available online at www.sciencedirect.com
SCIENCE DIRECT®
Journal of Chromatography A, 1023 (2004) 49–56
JOURNAL OF CHROMATOGRAPHY A
www.elsevier.com/locate/chroma

Chemical characterisation of different separation media based on agarose by static time-of-flight secondary ion mass spectrometry

Bo-Lennart Johansson[a,*], Mikael Andersson[a], Jukka Lausmaa[b], Peter Sjövall[b]

[a] *Research and Development, Amersham Biosciences AB, SE-751 84 Uppsala, Sweden*
[b] *Department of Chemistry and Materials Technology, SP Swedish National Testing and Research Institute, Box 857, SE-750 15 Borås, Sweden*

Received 23 January 2003; received in revised form 21 May 2003; accepted 6 October 2003

Abstract

In this paper, the novel application of time-of-flight secondary ion mass spectrometry (TOF-SIMS) for qualitative and semi-quantitative investigation of the surface chemistry of separation media based on beaded agarose is reported. Five different media were studied: DEAE Sepharose™ Fast Flow, Q Sepharose Fast Flow, SP Sepharose Fast Flow, Phenyl Sepharose Fast Flow at ligand densities between 7 and 33% (w/w) and the base matrix Sepharose 6 Fast Flow. The obtained TOF-SIMS spectra reveal significant chemical information regarding the ligands (DEAE, Q, SP and Phenyl) which are covalently attached to the agarose-based matrix Sepharose 6 Fast Flow. For the anion-exchange media (DEAE and Q Sepharose Fast Flow), the positive TOF-SIMS spectra yielded several strong characteristic fragment peaks from the amine ligands. Structural information was obtained, e.g. from the peak at *m/z* 173.20, originating from the ion structure $[(C_2H_5)_2NCH_2CH_2NH(C_2H_5)_2]^+$, which shows that the ligand in DEAE Sepharose Fast Flow is composed of both tertiary and quaternary amines. The positive spectrum of Phenyl Sepharose Fast Flow contained major fragments both from the base matrix and the ligand. The cation-exchanger (SP Sepharose Fast Flow) gave rise to a positive spectrum resembling that of the base matrix (Sepharose 6 Fast Flow) but with a different intensity pattern of the matrix fragments. In addition, peaks with low intensity at *m/z* 109.94, 125.94 and 139.95 corresponding to $Na_2SO_2^+$, $Na_2SO_3^+$ and $Na_2SO_3CH_2^+$, respectively, were observed. The positive TOF-SIMS spectrum of Sepharose 6 Fast Flow contains a large number of fragments in the mass range up to *m/z* 200 identified as $C_xH_yO_z$ and C_xH_y structures. The results clearly show that positive TOF-SIMS spectra of different media based on Sepharose 6 Fast Flow are strongly influenced by the ligand coupled to the matrix. The negative TOF-SIMS spectra contained several ligand-specific, characteristic peaks for the cation-exchanger, having sulphonate as the ion-exchange group. Negative fragments such as S^-, SO^-, SO_2^-, SO_3^-, $C_2H_3SO_3^-$, $C_3H_5SO_3^-$ and $OC_3H_5SO_3^-$ were observed. Phenyl Sepharose Fast Flow, which has an uncharged group (Phenyl) coupled to the agarose matrix yielded one ligand-related peak corresponding to the $C_6H_5O^-$ fragment. DEAE and Q ligands could only be identified by the appearance of the fragments CN^- and CNO^- in the negative spectrum. However, a strong peak corresponding to the counter ion (Cl^-) was observed. TOF-SIMS analysis can also be used for the investigation of residues from the coupling procedure that bonds the ligands to the matrix. One example is the observation of bromine peaks in the negative spectrum of Q Sepharose Fast Flow. Furthermore, it has also been shown that different ligand concentrations of Phenyl Sepharose Fast Flow can easily be detected by TOF-SIMS analysis. Information regarding the difference between the ligand density on the surface of the beads and in the bulk can also be obtained. However, spectra registered on the outermost surface and on the pore surface (crushed beads) of DEAE Sepharose Fast Flow clearly show that the agarose and the DEAE groups are homogeneously distributed in the beads.

Keywords: Ligands; Stationary phase, LC; Mass spectrometry; Sepharose

1. Introduction

Liquid chromatography is one of the most commonly used methods for the separation of molecules and over the past four decades it has proved to be an effective way to analyse and purify protein mixtures [1–4]. The rapid development of biotechnology and the requirements placed on the purity of biopharmaceutical products have drastically increased the importance of well-characterised separation media. The majority of studies of separation media have used chromatographic properties such as retention time, breakthrough capacity, efficiency, selectivity, ligand density, particle size, pore volume and surface area in the evaluation of the nature of separation media [5–10]. Early approaches for the

* Corresponding author. Tel.: +46-18-6120442.
E-mail address: bo-lennart.johansson@amersham.com (B.-L. Johansson).

0021-9673/$ – see front matter © 2003 Elsevier B.V. All rights reserved.
doi:10.1016/j.chroma.2003.10.008

investigation of chromatographic media were mainly focused on the chromatographic technique itself. In simplistic terms, the sample acts as a probe to derive fundamental information of the medium and the separation process. It is generally accepted that interactions between the sample and the medium take place exclusively on the outer few nanometres of the total sample interaction area of the chromatographic support. Therefore, it can be of great interest to apply non-chromatographic surface-specific measurements for the characterisation of the chemical structure of surface substituents. In the past years, a number of novel approaches has been used to study the surface chemistry of separation media. Different spectroscopic methods such as total internal reflection fluorescence (TIRF) [11], UV-Vis diffuse reflectance spectroscopy [12], Fourier transform infrared (FT-IR) techniques [13], Raman spectroscopy [14], confocal scanning laser microscopy [15], electron spin resonance spectroscopy (ESR) [16], NMR spectroscopy and magnetic resonance imaging [17,18] have been employed. These spectroscopic approaches give insight into, for example, the organisation, orientation, polarity, conformation and amount of immobilised groups on the surface of the separation medium, but none of them can be regarded as surface sensitive methods, since their probing depth is of the order of 1 μm or more. Highly surface sensitive techniques such as X-ray photoelectron spectroscopy (XPS) and static secondary ion mass spectrometry (SIMS) have also been used to study separation media, however, only silica-based ones [19,20]. These two techniques are surface sensitive on the scale 1–10 nm and therefore more sensitive to the chemistry of the chromatographic relevant surface than the above-mentioned methods. While XPS can give some limited chemical bonding information via chemical shifts in the measured binding energies of core level peaks, it is generally accepted that the characteristic fragmentation patterns and unique peaks in TOF-SIMS spectra have the potential for providing more specific and detailed chemical information, especially for organic materials.

In the present study, the use of TOF-SIMS for surface characterisation of agarose-based media for gel filtration, hydrophobic interaction chromatography, cation- and anion-exchange chromatography is evaluated. TOF-SIMS was used to investigate the molecular structure of the different ligands and to characterise the agarose matrix with respect to the positive and negative ion fragment distributions and the presence of trace elements on the surface.

2. Experimental

2.1. Materials

All chromatography media (Sepharose^{TM} Fast Flow base matrix, DEAE Sepharose Fast Flow, Phenyl Sepharose Fast Flow, Q Sepharose Fast Flow and SP Sepharose Fast Flow) were obtained from Amersham Biosciences (Uppsala, Sweden). Two Phenyl Sepharose Fast Flow media, with different ligand densities (HS: 40 μmol/ml; LS: 20 μmol/ml), were used. The high density medium was used if not otherwise stated. The sodium chloride was purchased from Merck (Darmstadt, Germany).

2.2. Sample preparation

Each chromatography medium was washed on a glass filter funnel; first in distilled water, then in 0.50 M NaCl solution and finally in distilled water. The media were then dried by suction to remove excess water and finally dried at 43 °C in a Speedvac evaporation system under vacuum conditions (down to 1 mbar). The sample treatment procedure leaves all beads intact and not crushed. However, in some experiments with DEAE Sepharose Fast Flow the dried sample was ground to crush the beads and thus making the pore surface available for analysis. This was done to verify that the bulk material of the beads is of the same composition as the outer surface of the beads.

2.3. TOF-SIMS analysis

TOF-SIMS spectra were recorded on a TOF-SIMS IV instrument (ION-TOF GmbH, Germany) using a 25 keV Ga^+ primary ion beam (0.5 A) and an analysis area of 200 μm × 200 μm. Charge compensation was achieved using a low energy electron flood gun. Due to the relatively high roughness of the sample surface (bead size 45–165 μm), and the insulating properties of the material, the mass resolution was improved retrospectively by extracting spectra from a limited part of the analysis area, such as a single or a few particles. The resulting mass resolution was typically 3000–4000.

For the TOF-SIMS analysis the sample particles were attached to a metal block using double-sided tape (3M, no. 665). Sample powder was placed on the tape, making sure that the entire tape surface was covered. A clean aluminium foil was gently pressed onto the tape in order to fix the powder onto the tape. The excess powder was removed from the sample surface by tilting the metal block and gently knocking it. The metal block was immediately mounted on the sample holder and introduced into the UHV chamber. TOF-SIMS spectra were also recorded from the clean tape surface for reference, in order to allow for exclusion of tape contribution to the spectra.

3. Results and discussion

SIMS has previously been used to characterise separation media based on silica and it was shown that correlation between surface analytical and chromatographic data from a range of alkyl-bonded silica (C1–C18) packing materials could be verified [20]. For example, correlation between the retention factor of a number of acidic, basic and neutral

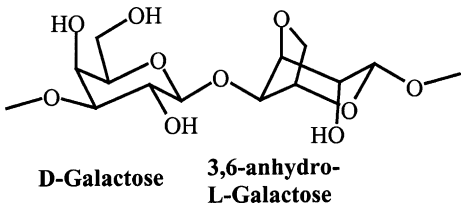

Fig. 1. Partial structure of agarose (alternating 1,3-linked β-D-galactose and 1,4-linked 3,6-anhydro-α-L-galactose).

solutes and SIMS alkyl:Si ion peak area ratios was obtained. In the present study we have focused on separation media based on the polysaccharide agarose (Fig. 1). The aim of this investigation was to study the TOF-SIMS response of different ligands covalently attached to agarose beads of a particle size of 45–165 μm (Sepharose 6 Fast Flow). The agarose gel structure is an open three-dimensional network of fibres composed of spontaneously aggregated galactan helices [21]. These have been cross-linked with epichlorohydrin to make the beads more rigid and physically stable. Two anion-exchangers (DEAE Sepharose Fast Flow and Q Sepharose Fast Flow), one cation-exchanger (SP Sepharose Fast Flow) and one medium aimed for hydrophobic interaction chromatography (Phenyl Sepharose Fast Flow) were analysed by TOF-SIMS. All these media are based on Sepharose 6 Fast Flow that also was analysed. The tentative chemical structures of the ligands [22] are presented in Fig. 2. The ligand density of DEAE, Q, SP and Phenyl Sepharose Fast Flow is about 0.13, 0.21, 0.21 and 0.04 mmol/ml, respectively, according to the manufacturer of the media. This means that the ligands of dried DEAE, Q, SP and Phenyl Sepharose Fast Flow media constitute 16, 33, 30 and 7% (w/w) of the total weight of the dried sample, respectively. The ligand surface density, in terms of ligands per cm^2 is, however, not known.

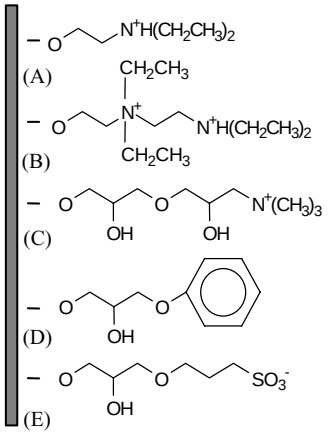

Fig. 2. Tentative ligand structures rationalised from the ligand coupling procedure. DEAE ligand (A) and the DEAE tandem group (B) of DEAE Sepharose Fast Flow, the Q ligand (C) of Q Sepharose Fast Flow, the Phenyl ligand (D) of Phenyl Sepharose Fast Flow and the SP ligand (E) of SP Sepharose Fast Flow.

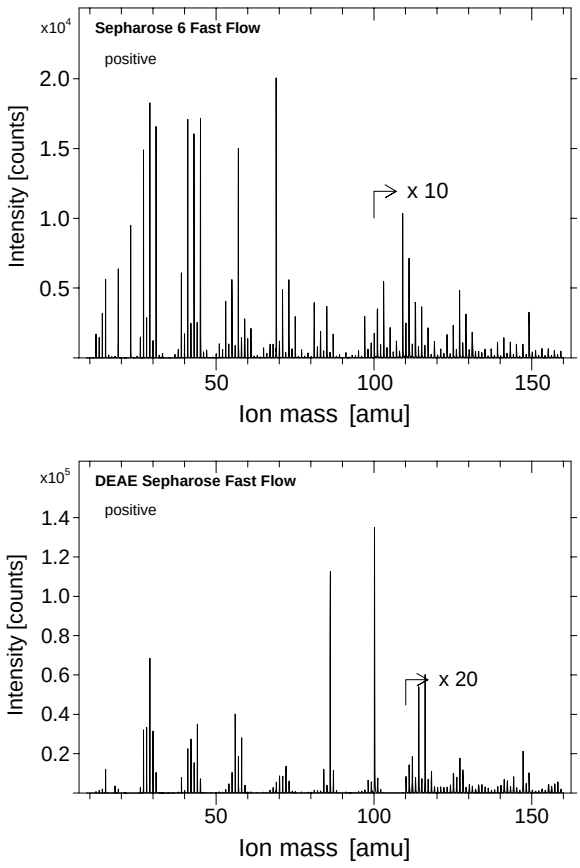

Fig. 3. Positive ion spectra of Sepharose 6 Fast Flow and DEAE Sepharose Fast Flow.

3.1. Positive spectra

Fig. 3 shows a typical example of a positive secondary ion mass spectrum from Sepharose 6 Fast Flow. The spectrum displays a range of prominent peaks at *m/z* values lower than 150, corresponding to fragments with $C_xH_yO_z$ and C_xH_y structures. The assignments of the 20 most prominent peaks are presented in Table 1. The spectrum of Sepharose 6 Fast Flow resembles that from agarose (not shown) indi-

Table 1
Summary of prominent positive ions in the TOF-SIMS spectrum of Sepharose 6 Fast Flow

Prominent positive ion peaks (*m/z*)	Structural assignments	Prominent positive ion peaks (*m/z*)	Structural assignments
15.02	CH_3^+	53.04	$C_4H_5^+$
27.02	$C_2H_3^+$	55.06	$C_4H_7^+$
29.00	CHO^+	55.02	$C_3H_3O^+$
29.04	$C_2H_5^+$	57.04	$C_3H_5O^+$
31.02	CH_3O^+	69.03	$C_4H_5O^+$
39.02	$C_3H_3^+$	71.01	$C_3H_3O_2^+$
41.04	$C_3H_5^+$	73.03	$C_3H_5O_2^+$
43.02	$C_2H_3O^+$	81.04	$C_5H_5O^+$
43.06	$C_3H_7^+$	85.03	$C_4H_5O_2^+$
45.03	$C_2H_5O^+$	97.03	$C_5H_5O_2^+$

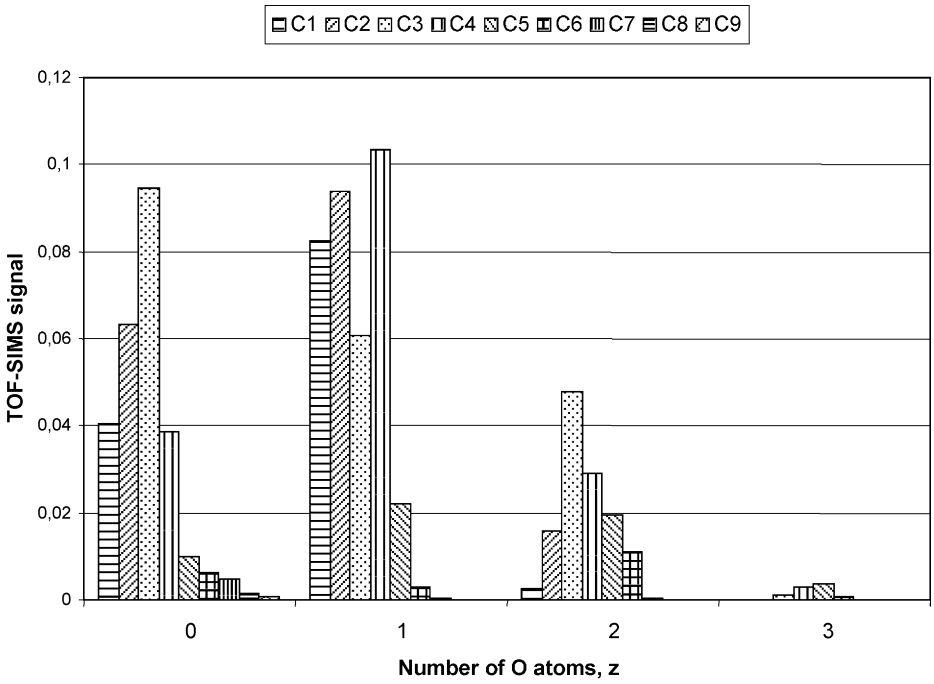

Fig. 4. $C_xH_yO_z^+$ fragment distribution in TOF-SIMS spectra from agarose.

cating that the surface molecular structure of Sepharose 6 Fast Flow resembles that of agarose. The diagram in Fig. 4 shows the distribution of $C_xH_yO_z$ fragments in the positive TOF-SIMS spectrum for agarose. The diagram shows that fragments containing one to four carbons and zero or one oxygen dominate the spectrum and that the number of fragments containing oxygen decreases with the number of oxygen atoms. A more comprehensive interpretation of the TOF-SIMS spectra of agarose and Sepharose media with different degrees of cross-linking and pore size distribution will be presented in a forthcoming article.

The modification of the base matrix (Sepharose 6 Fast Flow) with positively charged amines (Fig. 2A–C) or an uncharged hydrophobic ligand (Fig. 2D) can easily be detected by the appearance of positive ligand ion fragments in the spectrum.

The TOF-SIMS spectrum of DEAE Sepharose Fast Flow (Fig. 3 and Table 2) contains high intensity characteristic peaks from the ligand (Fig. 2A and B). Although the DEAE ligands only correspond to about 16% (w/w) of the total weight of the medium they dominate the positive ion spectrum. This indicates that the ligands are overrepresented at the surface of the beads or that the amine ligands are more easily fragmented to positive ions than the base matrix (see further). The production of DEAE Sepharose Fast Flow is accomplished by using the reaction of diethylaminoethyl chloride with agarose under alkaline conditions. This reaction gives rise to single substituents of the type presented in Fig. 2A and also the "tandem" substituents shown in Fig. 2B [23]. The positive ion fragments containing two nitrogen atoms (Table 2) clearly show that DEAE tandem groups (Fig. 2B) exist at the surface of this medium. For example, the peak corresponding to *m/z* 173.20 is due to the ion structure $[(C_2H_5)_2NCH_2CH_2NH(C_2H_5)_2]^+$. The two major positive ligand fragments occurred at *m/z* 86.10 ($[CH_2N(C_2H_5)_2]^+$) and 100.12 ($[CH_2CH_2N(C_2H_5)_2]^+$) which shows that the ligands are preferably fragmented one or two methylene groups away from the tertiary amine group. These fragments can be generated from either of the two DEAE ligand structures (Fig. 2A and B). The observation of positive ions such as $C_6H_{14}NO^+$ (*m/z* 116.11) and $C_8H_{20}N_2O^+$ (*m/z* 160.13) also indicates that the ligand of DEAE Sepharose Fast Flow is attached to the agarose beads via an ether bond. Furthermore, the peak at *m/z* 29.04 (corresponding to the ion $C_2H_5^+$) exhibits a much higher relative intensity compared to Sepharose 6 Fast Flow, indicating that the amine groups are substituted by C_2H_5 groups.

The samples where DEAE Sepharose Fast Flow was crushed exhibited no significant difference in the spectrum

Table 2
Summary of major positive ions in the TOF-SIMS spectrum of DEAE Sepharose Fast Flow

Prominent positive ion peaks (*m/z*)	Structural assignments	Prominent positive ion peaks (*m/z*)	Structural assignments
27.02	$C_2H_3^+$	72.08	$C_4H_{10}N^+$
28.02	CH_2N^+	84.08	$C_5H_{10}N^+$
29.04	$C_2H_5^+$	86.10	$C_5H_{12}N^+$
30.04	CH_4N^+	87.10	$C_5H_{13}N^+$
42.03	$C_2H_4N^+$	100.12	$C_6H_{14}N^+$
44.05	$C_2H_6N^+$	116.11	$C_6H_{14}NO^+$
56.05	$C_3H_6N^+$	127.12	$C_7H_{15}N_2^+$
58.07	$C_3H_8N^+$	160.13	$C_8H_{20}N_2O^+$
70.07	$C_4H_8N^+$	173.20	$C_{10}H_{25}N_2^+$

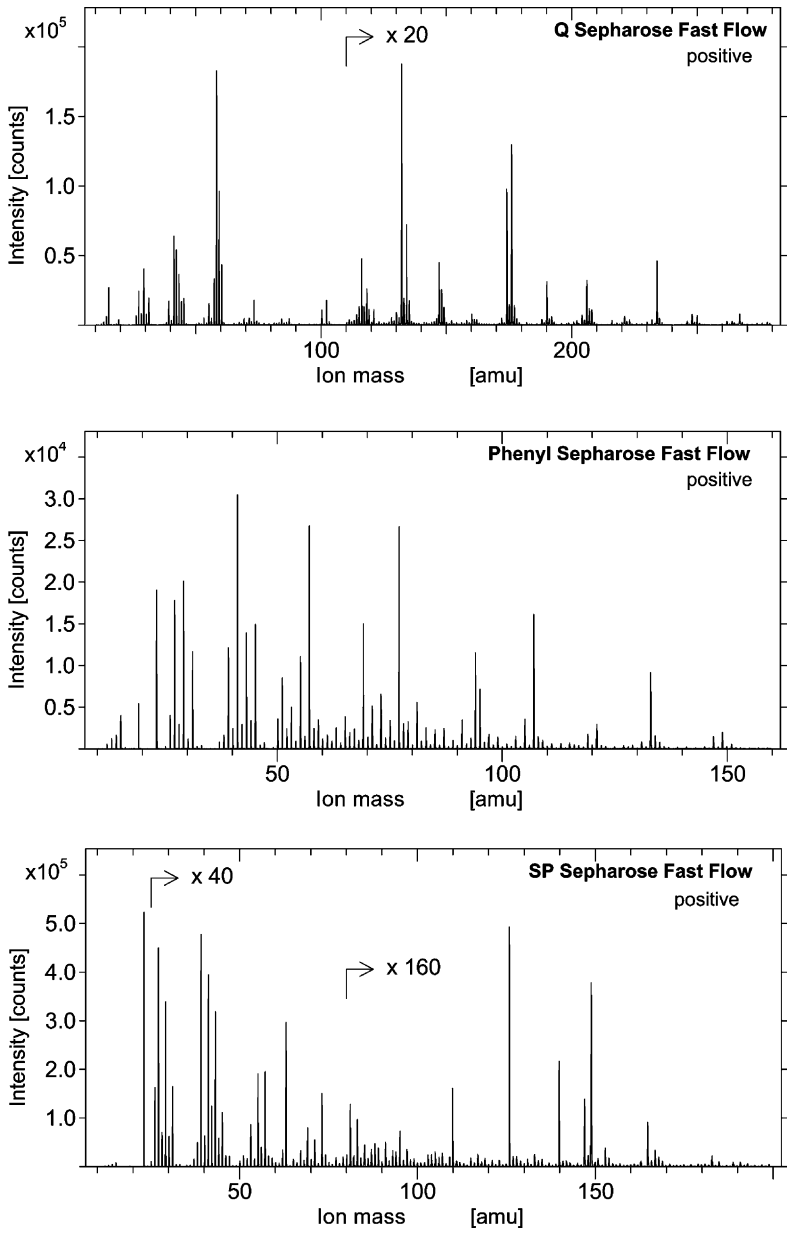

Fig. 5. Positive ion spectra of Q Sepharose Fast Flow, Phenyl Sepharose Fast Flow and SP Sepharose Fast Flow.

compared to uncrushed material. Furthermore, the ratio of the intensities of the DEAE peaks to Sepharose-related peaks is the same. These results clearly indicate that DEAE groups and the agarose structure are homogeneously distributed in the beads.

In the positive spectrum of Q Sepharose Fast Flow (Fig. 2C), all main peaks originate from the ligand (Fig. 5 and Table 3). The two largest ion peaks are $[CH_2N(CH_3)_2]^+$ (*m*/*z* 58.07) and $[N(CH_3)_3]^+$ (*m*/*z* 59.07). These peaks give a clear verification of the structure of the ion-exchange group in Q Sepharose Fast Flow. Furthermore, the whole ion-exchange spacer structure presented in Fig. 2C can be deduced. For example, the observed positive ion $C_9H_{20}NO_4^+$ (*m*/*z* 206.14) represents the total ligand structure in Fig. 2C except for the loss of one proton in the

Table 3
Summary of positive ions containing nitrogen in the TOF-SIMS spectrum of Q Sepharose Fast Flow

Prominent positive ion peaks (*m*/*z*)	Structural assignments	Prominent positive ion peaks (*m*/*z*)	Structural assignments
42.03	$C_2H_4N^+$	132.10	$C_6H_{14}NO_2^+$
58.07	$C_3H_8N^+$	174.15	$C_9H_{20}NO_2^+$
59.07	$C_3H_9N^+$	176.13	$C_8H_{18}NO_3^+$
60.09	$C_3H_{10}N^+$	190.15	$C_9H_{20}NO_3^+$
100.11	$C_6H_{14}N^+$	206.14	$C_9H_{20}NO_4^+$
102.09	$C_5H_{12}NO^+$	234.17	$C_{11}H_{24}NO_4^+$
116.11	$C_6H_{14}NO^+$		

Table 4
Summary of prominent positive ions in the TOF-SIMS spectrum of Phenyl Sepharose Fast Flow

Prominent positive ion peaks (*m/z*)	Structural assignments	Prominent positive ion peaks (*m/z*)	Structural assignments
27.02	$C_2H_3^+$	69.03	$C_4H_5O^+$
31.02	CH_3O^+	77.04	$C_6H_5^+$
29.04	$C_2H_5^+$	94.04	$C_6H_6O^+$
39.03	$C_3H_3^+$	95.05	$C_6H_7O^+$
41.04	$C_3H_5^+$	107.05	$C_7H_7O^+$
43.02	$C_2H_3O^+$	121.06	$C_8H_9O^+$
57.04	$C_3H_5O^+$	133.07	$C_9H_9O^+$

fragmentation process. In addition, the fragment at *m/z* 234.17 represents the ion $[C_{11}H_{24}NO_4]^+$, representing the whole ligand in Fig. 2C, plus C_2H_4 from the agarose matrix. Furthermore, positive ion fragments containing one atom of nitrogen and zero to four atoms of oxygen (Table 3) represent fragments of the total ligand structure in Fig. 2C.

The ligand structure of Phenyl Sepharose Fast Flow, in which an uncharged Phenyl ligand has been coupled via the reaction of phenyl glycidyl ether with Sepharose 6 Fast Flow [24], is depicted in Fig. 2D. Compared to the other investigated media, the ligand concentration of Phenyl Sepharose Fast Flow is about five times lower. The positive ion spectrum of Phenyl Sepharose Fast Flow (Fig. 5) shows major peaks both from the agarose matrix and the ligand (Table 4). Comparison of the TOF-SIMS spectrum of Phenyl Sepharose Fast Flow (Fig. 5) and the spectrum of Sepharose 6 Fast Flow reveals that five major positive peaks are obtained from the ligand. These aromatic peaks are located at *m/z* 77.04 ($C_6H_5^+$), 94.04 ($C_6H_6O^+$), 107.05 ($C_7H_7O^+$), 121.06 ($C_8H_9O^+$) and 133.07 ($C_9H_9O^+$), respectively. These peaks are in accordance with the structure of the ligand presented in Fig. 2D. Minor ligand fragments were also observed at *m/z* 78.04 ($C_6H_6^+$), 79.05 ($C_6H_7^+$) and 105.07 ($C_8H_9^+$). However, no significant positive ion fragments with two or three oxygen atoms and with more than seven carbon atoms were detected from the ligand.

To test the possibility of detecting differences in ligand density, two Phenyl Sepharose Fast Flow media with a ligand content of 40 and 20 μmol/ml, respectively, were analysed. The spectra were normalised to the intensity of the $C_3H_5^+$ peak and the ratios of the positive ligand fragments of both media were calculated after correction of the base matrix contribution (Sepharose 6 Fast Flow). The results (Table 5) show that Phenyl Sepharose Fast Flow HS resulted in three to four times higher normalised ligand ion intensities compared to Phenyl Sepharose Fast Flow LS (Table 5). The corresponding bulk ratio, as determined by UV measurements after hydrolysis of the medium [24], is 2. It is well known that secondary ion yields can be dramatically influenced by matrix effects, and it cannot be excluded that such effect contribute to the observed differences between the media with low and high degree of substitution.

The medium based on a sulphonic acid ligand, SP Sepharose Fast Flow (ligand E), showed a very strong peak from the Na^+ counter ion (Fig. 5). Furthermore, the SP groups change the fragmentation of the agarose base matrix, compared to the results obtained from Sepharose Fast Flow, so that less positive fragments with the generic formula $C_xH_yO_z$ ($x = 4$–6) are formed. In addition, peaks with low intensity at *m/z* 109.94, 125.93 and 139.95 corresponding to $Na_2SO_2^+$, $Na_2SO_3^+$ and $Na_2SO_3CH_2^+$, respectively, were observed (Fig. 5).

3.2. Negative spectra

In general, the negative ion spectra contain less characteristic peaks compared to the positive ion spectra. In Fig. 6, negative spectra of Sepharose 6 Fast Flow, SP and Phenyl Sepharose Fast Flow are depicted. The negative spectra from SP Sepharose Fast Flow (Fig. 2, ligand E) yielded strong signals from fragments such as S^- (*m/z* 31.97), SO^- (*m/z* 47.97), SO_2^- (*m/z* 63.96) and SO_3^- (*m/z* 79.96), clearly showing that the cation-exchanger has a sulphonic acid ligand. Furthermore, small peaks corresponding to $C_2H_3SO_3^-$, $C_3H_5SO_3^-$ and $OC_3H_5SO_3^-$ reveal more structural features of the ligand. The negative spectrum of Phenyl Sepharose Fast Flow shows a prominent peak at *m/z* 93.07, which

Table 5
Intensity ratios of ligand-specific positive fragments of Phenyl Sepharose Fast Flow with high (HS) and low substitution (LS)

Ion peaks (*m/z*)	Structural assignments	Corrected intensities (normalised to $C_3H_5^+$ signal)			Intensity ratio[a]
		Phenyl Sepharose Fast Flow (HS)	Phenyl Sepharose Fast Flow (LS)	Sepharose 6 Fast Flow (ZS)	
41.04	$C_3H_5^+$	100	100	100	NA
77.04	$C_6H_5^+$	78.55	25.19	2.79	3.38
78.04	$C_6H_6^+$	13.90	4.95	0.64	3.08
94.04	$C_6H_6O^+$	36.23	12.91	0.79	2.92
105.07	$C_8H_9^+$	7.73	3.20	0.80	2.89
107.05	$C_7H_7O^+$	53.04	12.86	0.56	4.27
121.06	$C_8H_9O^+$	13.32	3.76	0.31	3.77

The intensities are normalised to the $C_3H_5^+$ signal and the intensity ratio is corrected for the contribution of the base matrix (Sepharose 6 Fast Flow, zero substitution (ZS)). NA: not applicable.
[a] (HS − ZS)/(LS − ZS).

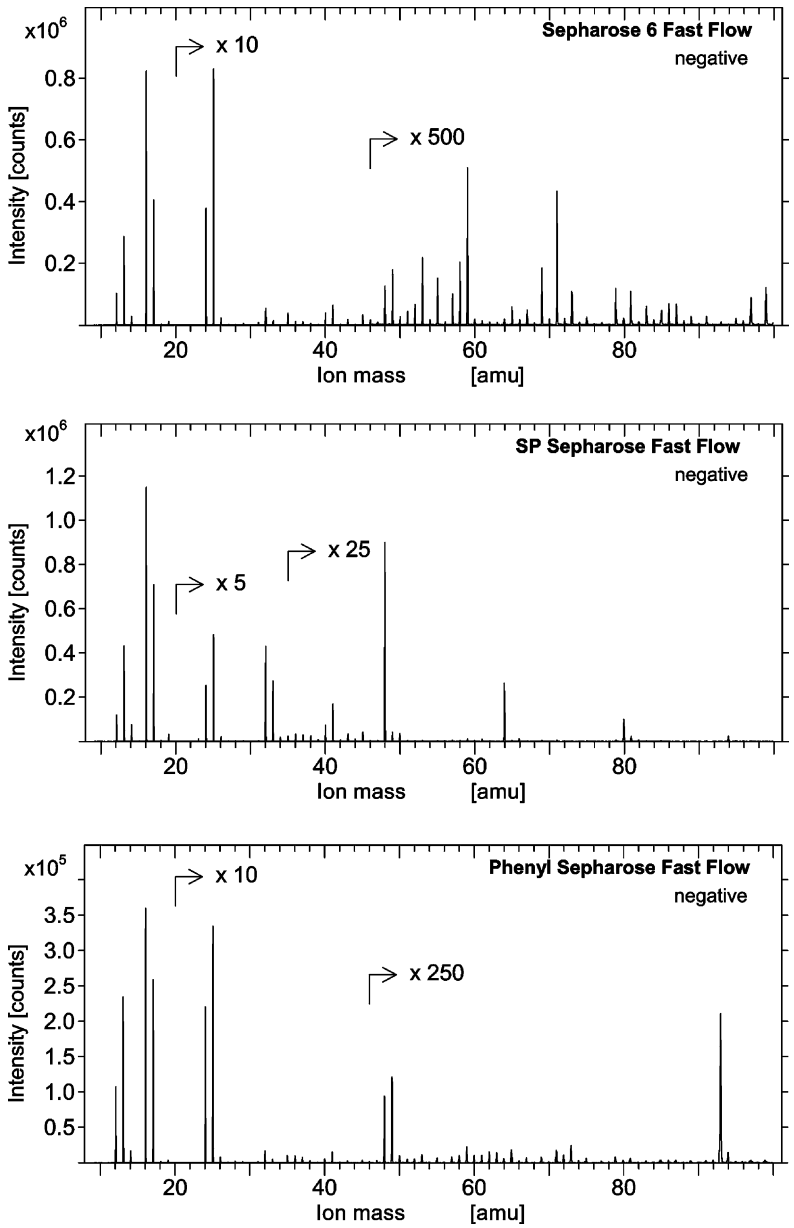

Fig. 6. Negative ion spectra for Sepharose 6 Fast Flow, SP Sepharose Fast Flow and Phenyl Sepharose Fast Flow.

corresponds to the negative ligand fragment $C_6H_5O^-$. The anion-exchangers DEAE and Q Sepharose Fast Flow yielded spectra resembling that of the base matrix, except for a prominent peak of the counter ion (Cl^-) and small peaks from CN^- and CNO^- fragments. These results, and those obtained from positive TOF-SIMS spectra, which were dominated by ligand fragments (see earlier), strongly indicate that the surfaces of the studied anion-exchangers are composed of both ligands and agarose. The ions CN^- and CNO^- were the only nitrogen containing ligand-specific fragments observed in negative TOF-SIMS spectra of DEAE and Q Sepharose Fast Flow. Furthermore, peaks from $^{79}Br^-$ and $^{81}Br^-$ were observed in the spectrum of Q Sepharose Fast Flow indicating that small amounts of bromine atoms from the synthesis procedure (bromination of allyl groups) in the coupling procedure of the anion-exchange group remain on the agarose matrix.

4. Conclusions

This study demonstrates the significant potential of TOF-SIMS to reveal detailed information regarding the chemistry and composition of ligands attached to agarose-based beads. Positive ion TOF-SIMS spectra of separation media based on cross-linked Sepharose beads (Sepharose 6 Fast Flow) resulted in low-mass fragments below *m*/*z* 200. These ions are specific for the base matrix

and the ligands attached to the beads. The amount of structural information obtained from positive TOF-SIMS data on ligands covalently attached to Sepharose 6 Fast Flow beads varies with the type of ligand in the order: anion-exchange ligand > hydrophobic uncharged ligand > cation-exchange ligand.

Positive TOF-SIMS spectra are best suited for structural evaluation of anion-exchange ligands composed of positively charged amines. These ligands are easily fragmented and the resulting spectra are dominated of ions emanating from the ligands. Identification of fragments, such as $[(C_2H_5)_2NCH_2CH_2NH(C_2H_5)_2]^+$ from DEAE Sepharose Fast Flow, has shown that tandem groups are formed during the coupling of the ligand to the beads. In the case of the hydrophobic medium Phenyl Sepharose Fast Flow, the positive TOF-SIMS spectrum contains major peaks both from the base matrix and the aromatic ligand. The positive TOF-SIMS spectrum of SP Sepharose Fast Flow showed an intense peak of the counter ion to the cation-exchange ligand. Furthermore, minor positive peaks from $Na_2SO_2^+$, $Na_2SO_3^+$ and $Na_2SO_3CH_2^+$ fragments reveal significant information of the ligand structure.

In negative TOF-SIMS spectra of SP Sepharose Fast Flow, the observed fragments $C_2H_3SO_3^-$, $C_3H_5SO_3^-$ and $OC_3H_5SO_3^-$ made it possible to make a more comprehensive identification, compared to positive TOF-SIMS, of the chemical composition of the cation-exchange ligand ($-OCH_2CH_2CH_2SO_3^-$). One ligand-specific fragment ($C_6H_5O^-$) in negative TOF-SIMS spectra was also obtained from Phenyl Sepharose Fast Flow. However, the anion-exchangers gave no fragments in negative TOF-SIMS spectra useful for assignment of the structure of the ligand. A strong peak from the counter ion (Cl^-) was observed, though.

The presented results prove that both positive and negative TOF-SIMS spectra can be used to get structural information of the base matrix as well as the ligand structure of different separation media based on Sepharose 6 Fast Flow. Ligand-specific, characteristic fragments are easily generated from anion-exchangers in the positive spectra, while from cation-exchangers, the negative spectra provide more structural information.

References

[1] G. Sofer, J. Chromatogr. A 707 (1995) 23.
[2] J.-C. Jansson, T. Petersson, in: G. Ganetsos, P.E. Barker (Eds.), Preparative and Production Scale Chromatography, Marcel Dekker, New York, 1992, pp. 559–590.
[3] K.K. Unger, R. Janzen, J. Chromatogr. 373 (1986) 227.
[4] J.-C. Jansson, L. Rydén, Protein Purification—Principles, High Resolution Methods and Applications, VCH Publishers, New York, 1989.
[5] J.A. Perry, T.J. Szczerba, J. Chromatogr. 484 (1989) 267.
[6] E. Boschetti, J. Chromatogr. A 658 (1994) 207.
[7] K. Kimata, K. Iwaguchi, S. Onishi, K. Jinno, R. Eksteen, K. Hosoya, M. Araki, N. Tanaka, J. Chromatogr. Sci. 27 (1989) 721.
[8] D. Wu, R.R. Walters, J. Chromatogr. 598 (1992) 7.
[9] P.R. Levision, C. Mumford, M. Streater, A. Brandt-Nielsen, N.D. Pathirana, S.E. Badger, J. Chromatogr. A 760 (1995) 151.
[10] H. Engelhardt, H. Löw, W. Götzinger, J. Chromatogr. 544 (1991) 371.
[11] V.M. Rangnekar, P.B. Oldham, Anal. Chem. 62 (1990) 1144.
[12] S.C. Rutan, J.M. Harris, J. Chromatogr. A 656 (1993) 197.
[13] B.R. Suffolk, R.K. Gilpin, Anal. Chem. 57 (1985) 596.
[14] M. Ho, M. Cai, J.E. Pemberton, Anal. Chem. 69 (1997) 2613.
[15] A. Ljunglöf, M. Larsson, K.-G. Knuuttila, J. Lindgren, J. Chromatogr. A 893 (2000) 235.
[16] R.K. Gilpin, A. Kasturi, E. Gelerinter, Anal. Chem. 59 (1987) 1177.
[17] S. Chen, F. Qin, A.T. Watson, AIChE J. 40 (1994) 1238.
[18] L.F. Gladden, M.P. Hollwand, P. Alexander, AIChE J. 41 (1995) 894.
[19] V.A. Brown, D.A. Barett, P.N. Shaw, M.C. Davies, H.J. Ritchie, P. Ross, A.J. Paul, J.F. Watts, Surf. Interface Anal. 21 (1994) 263.
[20] D.A. Barrett, V.A. Brown, M.C. Davies, P.N. Shaw, Anal. Chem. 68 (1996) 2170.
[21] J.-C. Jansson, T. Kristiansen, in: K.K. Unger (Ed.), Packings and Stationary Phases in Chromatographic Techniques, Marcel Dekker, New York, 1990, pp. 747–781.
[22] J.-C. Jansson, L. Rydén, Protein Purification—Principles, High Resolution Methods and Applications, VCH Publishers, New York, 1989, pp. 116, 216.
[23] L. Ahrgren, A. de Belder, S.-O. Larsson, T. Mälson, in: E.J. Goethals (Ed.), Polymeric Amines and Ammonium Salts, Pergamon Press, New York, pp. 293–294.
[24] B.-L. Johansson, I. Drevin, J. Chromatogr. 391 (1987) 448.